water

MDPI

Article

Influence of Check Dams on Flood and Erosion Dynamic Processes of a Small Watershed in the Loss Plateau

Shuilong Yuan [1], Zhanbin Li [1,2], Peng Li [1], Guoce Xu [1,*], Haidong Gao [1], Lie Xiao [1], Feichao Wang [1] and Tian Wang [1]

[1] State Key Laboratory of Eco-Hydraulics in Northwest Arid Region of China, Xi'an University of Technology, Xi'an 710048, China; yuanshuilong@163.com (S.Y.); zhanbinli@126.com (Z.L.); lipeng74@163.com (P.L.); hdgao@msn.cn (H.G.); xiaosha525@163.com (L.X.); wangfeichao_0120@163.com (F.W.); wthuanjing@163.com (T.W.)

[2] State Key Laboratory of Soil Erosion and Dry-Land Farming on the Loess Plateau, Institute of Soil and Water Conservation, Chinese Academy of science and Ministry of Water Resources, Yangling 712100, China

* Correspondence: xuguoce_x@163.com; Tel./Fax: +86-29-8231-2651

Received: 21 March 2019; Accepted: 15 April 2019; Published: 19 April 2019

check for updates

Abstract: As an important soil and water conservation engineering measure, check dams have been constructed on a large scale in the Loess Plateau of China. However, their effects on runoff and sediment processes in the basin are still unclear. In this study, the hydrodynamic processes of the Wangmaogou watershed located in the Loess Plateau were simulated, and the influence of check dams on the flood and erosion dynamic processes in this watershed were also evaluated. The results showed that the check dams obviously reduced the flood peak and flood volume and mitigated the flood process. After the dam system was completed, the flood peak and flood volume were reduced by 65.34% and 58.67%, respectively. The erosion dynamic distribution of the main channel in the small watershed was changed to different extents by the different dam type combinations, and the erosion dynamic parameters of the channel decreased most after the dam system was completed, when the velocity and runoff shear stress of the outlet section were reduced by 10.69% and 31.08%, respectively. Additionally, the benefits of sediment reduction were most obvious after the check dam system was completed, with the sediment discharge in the watershed being reduced by 83.92%. The results of this study would provide specific implications for construction and management of check dams in the Loess plateau.

Keywords: check dam; flood; erosion dynamics; sediment reduction; hydrodynamic model

1. Introduction

The Chinese Loess Plateau is an area of about 650 thousand km^2 located in the middle and upper reaches of the Yellow River [1]. This region is well known for its severe soil erosion and high sediment yields from its most erosion-prone area of approximately 472 thousand km^2, including 91.2 thousand km^2 with sediment yields exceeding 8000 t/km^2/a [2]. This region has the most serious documented soil erosion rates in the world [3]. Soil erosion on the Loess Plateau has depleted land resources, degraded the environment, and caused severe river bed sedimentation along the lower reaches of the Yellow River, threatening the safety of local inhabitants [4]. Therefore, soil loss management and environmental protection are critical issues in the region [5]. Check dams are the most widely applied engineering structures for soil and water conservation in the erodible regions of the Loess Plateau, and they have been widely constructed to retain floodwater, intercept soil sediment, improve gully slope stabilities, and increase farmland [6–9]. Indeed, about 110,000 check dams were constructed by 2002, and this number is set to double by 2020 as part of a project launched by the Chinese Ministry of Water Resources [10]. Check dams are also often used in other countries, such as Ethiopia [11], Spain [12,13], Iran [14], Italy [15], and Mexico [16].

The performance of check dams for sediment and runoff control has been investigated in different studies, some of which are reviewed in the following. Check dams are constructed across gullies to reduce the velocity of concentrated water flows, reduce erosion, control sediment, and stabilize gullies [17,18]. The annual runoff was reduced by less than 14.3% by check dams in the Yanhe watershed [19]. Check dams also reduced the sediment load in the Rogativa catchment of Spain by approximately 77% [20]. A series of check dams have been built along waterways, and these have provided dense vegetation, stabilized the channels and considerably decreased the volume of sediments washed from the watershed [21]. Check dams are also found to modify water and sediment transport by impounding storm flow, reducing its velocity and peak rate, decreasing channel slope, and allowing more time for infiltration and sediment settling [22]. The construction of check dams is one of the most effective methods to control gully erosion and reduce sediment transport through field investigations [23]. The effects of check dams on scour dynamics vary greatly depending on initial slope, soil texture, spacing, drop height, and flow depth [24]. The effectiveness of sediment retention by check dams can be associated with different factors such as check dam characteristics, gully characteristics, and water flow conditions [25]. Accordingly, various studies have evaluated the impacts of check dams on controlling runoff, erosion, and sediment transfer [26–28].

Most studies conducted to date have focused on the effects of check dams on runoff and sediment, while few have explored the effects of check dams on floods and their erosion dynamic processes in small watersheds [17–20]. Different types of check dams have different effects on runoff and its erosion dynamic process; accordingly, it is important to identify the roles of different types of check dams. The main goals of the present study were to reveal the mechanisms by which check dams influence floods and their erosion dynamic process, and evaluate the sediment reduction benefits of different dam type combinations. Our specific objectives were to: (1) investigate the influence of different types of check dams and their combinations on the flood process of small watersheds; (2) explore the influence of different types of check dams and their combinations on the erosion dynamic processes in a small watershed; and (3) calculate the sediment reduction benefit of different types of check dam combinations.

2. Data and Methods

2.1. Study Area

The study was conducted in the Wangmaogou watershed (110°20′26′′–110°22′46′′E, 37°34′13′′–37°36′03′′N), which is located in the Loess Plateau of China. The Wangmaogou watershed is located in Suide County, Shaanxi Province, which belongs to the third-grade branch ditch of the Wuding River. The watershed covers an area of 5.97 km^2 and ranges in altitude from 936 to 1188 m. The main channel length is 3.75 km, and the average slope of the channel is 2.7% [29]. The watershed is characterized by a temperate semiarid continental monsoon climate with distinct seasons and large temperature differences. According to data from the soil and water conservation test station in Suide, the average annual temperature is 10.2 °C and the mean annual precipitation is approximately 513 mm, more than 60% of which occurs between July and September [30]. The study area is underlaid by loessial soil and rainfall during the flood season can result in serious soil erosion. As a well-studied watershed for soil and water conservation, many check dams have been implemented in the Wangmaogou watershed since the 1950s. Indeed, by the end of 2017 there were 23 normal check dams in Wangmaogou watershed, including two key dams, seven medium dams, and 14 small dams (Figure 1). The check dams were divided into three types: key dams, medium dams, and small dams. Key dams are composed of the dam body, spillway, and discharge structure; while middle dams are composed of a dam body and a discharge structure; and small check dams consists only of one dam body.

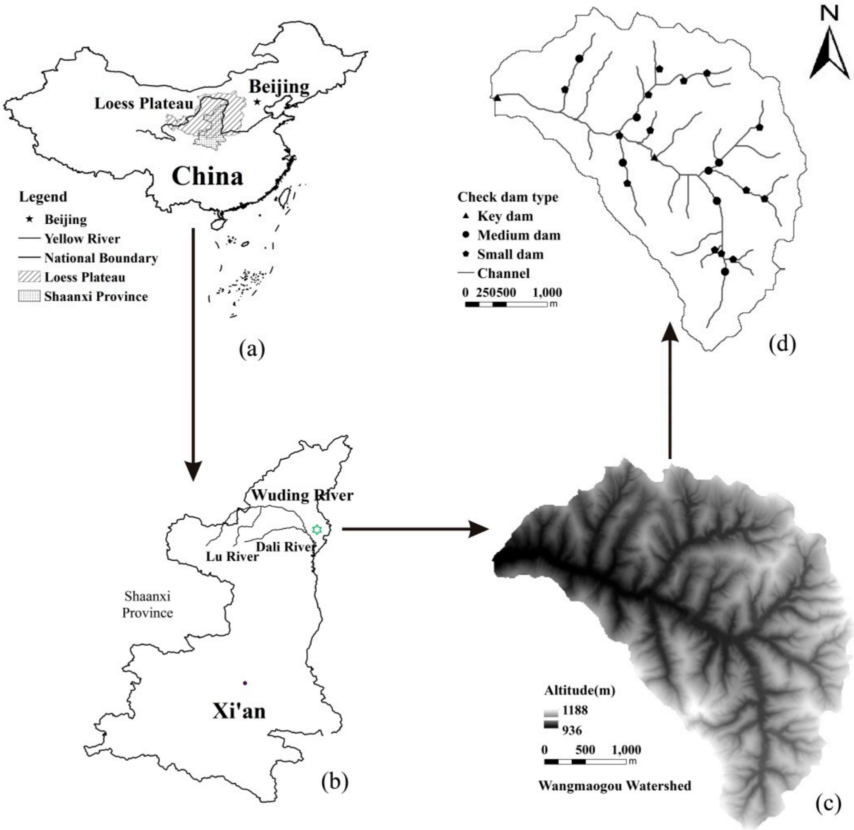

Figure 1. Location of the study area (**a**,**b**); the Wangmaogou watershed (**c**); and the layout of check dam types (**d**).

2.2. Data Sources

Runoff, sediment, and meteorological data were obtained from the Yellow River Water and soil Conservation Suide Supervision Bureau. The Suide Supervision Bureau established a watershed outlet hydrologic station in the Wangmaogou watershed. The station monitor runoff and sediment data from 1962 to 1966, mainly including water level, discharge, sediment concentration, and sediment transport rate. The terrain data is obtained from the State Bureau of Surveying and Mapping. The geodetic reference is the 1980 Xi'an coordinate system, contour distance of which is 5 m. The shape file is generated by paper maps via spatial registration after scanning, splicing, and manual tracking. The DEM with a resolution of 5 m is then generated by the Hutchinson method [31]. The land use data for the watershed was obtained from the land use survey of the Suide Supervision Bureau in 1960s. The channel section data utilized for the Mike 11 model (DHI, Copenhagen, Denmark) was extracted from the digital elevation model (DEM) with 5 m resolution using the 3D analyst tool in ArcGIS 10.1 (ESRI, California, America), then corrected based on field measurements. The geometric characteristics of check dams were obtained by field measurement, including dam length, dam height, dam width, and geometric size of the drainage structure.

2.3. Model Set Up

In this study, the channel hydrodynamic processes of the Wangmaogou watershed were simulated using the overland flow module of the distributed hydrological model MIKE SHE and the one-dimensional hydrodynamic model MIKE 11. First, the watershed scope was defined in the MIKE SHE model. The study area was discretized using a grid of 20 × 20 m, with a total of 29,700 grids. The study area DEM, with a 5 m resolution grid, was converted into a shape point terrain file by ArcGIS 10.1. The processed vector format digital elevation data file was directly imported into the model and interpolated by the triangle interpolation method, which sets the search radius to 20 m depending on the cell size. During the secondary torrential rain and flood, the evapotranspiration of the watershed is very small, so it can be ignored [32]. The precipitation data were transformed into a dfs0 file and imported into the model using the MIKE model software tools. The grid of the model is relatively large, so the land use types were divided into six categories according to the geomorphological characteristics of the study area: cultivated land, grassland, forest land, garden land, residential land, and traffic land. The overland flow module of the MIKE SHE model mainly contains three parameters: Manning number, detention storage, and initial water depth. The model deducts soil infiltration from precipitation data as precipitation input of the model. The amount of soil infiltration, which has an empirical value of 2 to 20 mm/h, mainly depends on the soil types, and the effects of vegetation are taken into account [33].

MIKE SHE and MIKE 11 were used to simulate overland flow and channel confluence processes, respectively. The river network vector file of the watershed was extracted from DEM with 5 m resolution using the ArcGIS 10.1 software and imported into the MIKE 11 model. The river network, which was automatically generated by the model, was manually modified according to the actual situation. The six river channels of the watershed are defined in the MIKE 11 model, and the check dams in the channel are expressed by the hydraulic structures in the river network file. The MIKE 11 model was coupled with the MIKE SHE model, and the storm flood model of the Wangmaogou watershed was established.

2.4. Calibration and Validation of the Model

The model of torrential rain and flooding in Wangmaogou watershed was calibrated by trial and error. The runoff process measured at the outlet of the watershed was selected as the calibration parameter. The model was calibrated based on two typical rainstorm flood processes, and was verified by another two rainstorm flood processes during the observation period. Theoretically, the parameters of the distributed watershed hydrological model can be obtained by experimental measurement, but the cell parameters of the model still need to be calibrated because of the difference between observation scale and simulation scale, the errors associated with experimental measurements, etc. [34,35]. At the same time, the distributed hydrological model should select as few parameters as possible when calibrating the model, because too many parameters may not improve the accuracy of the model, and the parameter calibration process will become extremely complex [36,37]. Therefore, fewer parameters were selected to calibrate the model in this study. Specifically, the parameters that need to be calibrated are detention storage, Manning number, leakage coefficient, and soil infiltration rate of different soil types. The performance of stream flow simulations was evaluated by comparing simulated and observed stream flow hydrographs through the following statistics: coefficient of determination (R^2) (Equation (1)) and Nash–Sutcliffe efficiency (NSE) (Equation (2)) [38,39].

$$R^2 = \left[\frac{\sum_{i=1}^{n} (O_i - \overline{O})(S_i - \overline{S})}{\sqrt{\sum_{i=1}^{n} (O_i - \overline{O})^2} \sqrt{\sum_{i=1}^{n} (S_i - \overline{S})^2}} \right]^2 \tag{1}$$

$$NSE = 1 - \frac{\sum_{i=1}^{n} (S_i - O_i)^2}{\sum_{i=1}^{n} (O_i - \overline{O})^2} \in (-\infty, 1] \tag{2}$$

where O_i is the simulated stream flow (m^3 s^{-1}), S_i is the observed stream flow (m^3 s^{-1}),$\overline{O}$ is the mean of the simulated stream flow (m^3 s^{-1}), and $\overline{S}$ is the mean of the observed stream flow (m^3 s^{-1}). Additionally, *NSE* indicates how well the plot of the observed value versus the simulated value fits the 1:1 line and ranges from 0 to 1, with higher values indicating better agreement.

2.5. Model Effect Evaluation

The erosion rainfall of small watersheds is mainly characterized by short duration and high intensity in the loess plateau. The four rainfall events selected in this study were the rain patterns with high frequency occurring in the Wangmaogou watershed from 1962 to 1966, which are good representations. We compared the observed and simulated flood processes during the calibration and validation periods (Figure 2). The results showed that there is good agreement between the simulated runoff and the observed runoff in the calibration and validation periods. This model can be used to simulate the dynamic changes in the flood process, which can be used for analysis of working conditions. The *NSE* values of the model were all higher than 0.8, the R^2 were 0.90 and 0.88, respectively, and the relative error of peak flow was only 1.72% and 3.33% in the calibration period. The *NSE* of the model was 0.60 and 0.71, respectively, the R^2 values were all 0.72, and the relative error of peak flow was only 11.05% and 12.05% in the validation period (Table 1). Simplification of model structure can cause model error [40]. The accuracy of the model in the validation period was lower than in the calibration period, which may have been because the model only couples the MIKE SHE overland flow module and MIKE 11. Generalization of the rainfall infiltration process is one of the reasons the accuracy of the model in the validation period is lower than that during the calibration period.

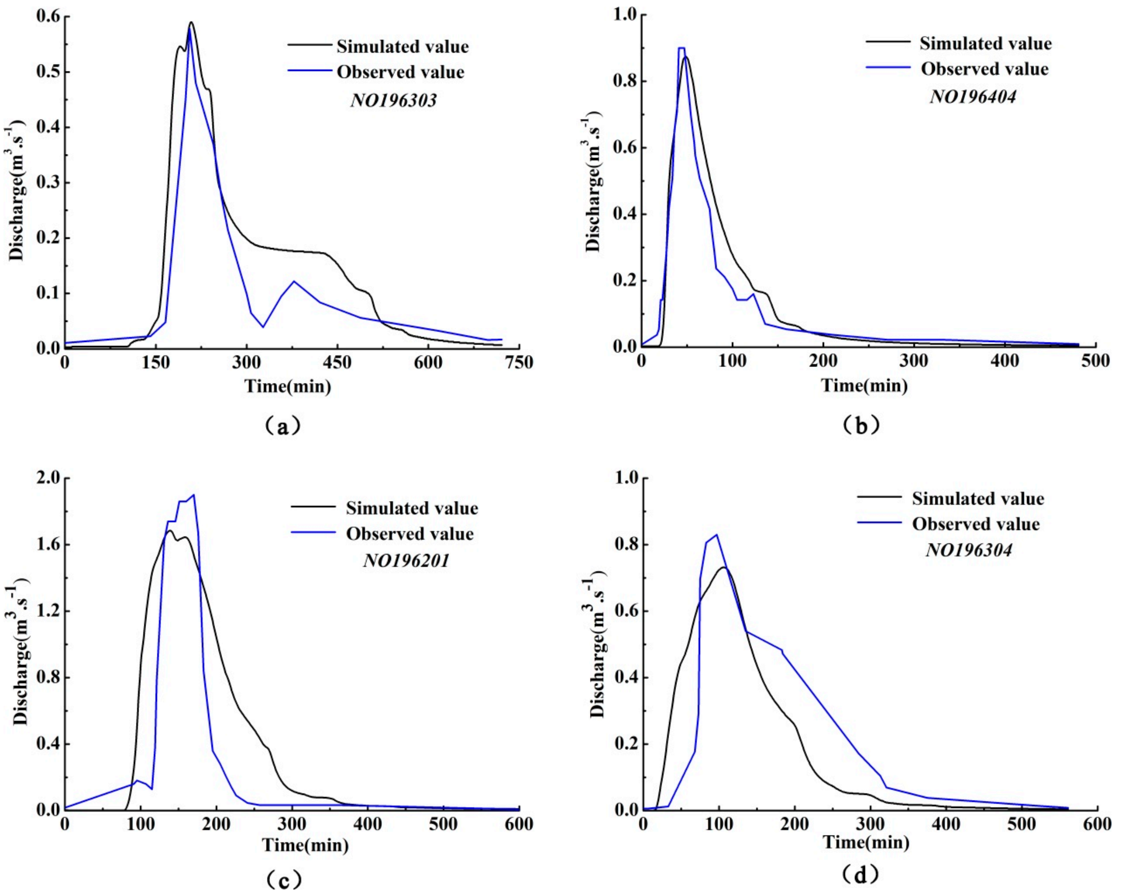

Figure 2. Model calibration results (**a**,**b**); model validation results (**c**,**d**).

Table 1. Model calibration and validation results of the Wangmaogou watershed.

Stage	Flood Number	Observed Value ($m^3 s^{-1}$)	Simulated Value ($m^3 s^{-1}$)	Relative Error/*Re* (%)	Determination Coefficient/R^2	Nash–Sutcliffe Coefficient /*NSE*
calibration	196303	0.58	0.59	1.72	0.90	0.80
	196404	0.90	0.87	3.33	0.88	0.85
validation	196201	1.90	1.69	11.05	0.72	0.60
	196304	0.83	0.73	12.05	0.72	0.71

2.6. Working Condition Design

In this study, the rainstorm flood process was simulated under different combinations of check dam types in a small watershed, and a total of eight different dam type combinations were designed (Table 2). N represents the case without dams; K represents the case with key dams only; M represents the case with medium dams only; S represents the case with small dams only; KM represents the case with key and medium dams; KS represents the case with key and small dams; KMZ represents the case with key, medium, and small dams.

Table 2. Working condition design of different dam type combinations.

Working Conditions	Coding	Different Dam Type Combinations in Watershed	Dam Name
1	N	No dams	——
2	K	Only key dams	Wangmaogou dam #1, Wangmaogou dam #2
3	M	Only medium dams	Huangbaigou dam #2, Nianyangou dam #1, Kanghegou dam #2, Sidizui dam #1, Madizui dam, Guandigou dam #1, Guandigou dam #4
4	S	Only small dams	Huangbaigou dam #1, Nianyangou dam #2, Nianyangou dam #3, Nianyangou dam #4, Kanghegou dam #1, Kanghegou dam #3, Sidizui dam #2, Wangtagou dam #1, Wangtagou dam #2, Guandigou dam #2
5	KM	Key and medium dam combination	——
6	KS	Key and small dam combination	——
7	MS	Medium and small dam combination	——
8	KMS	Key, medium, and small dam combination	——

2.7. Erosion Dynamic Parameter Calculation

(1) The construction of check dams has changed the connectivity of the channel. In this study, the formula used to calculate channel connectivity was constructed by referring to the formula for calculation of river connectivity [41], which was used to characterize the influence of the check dam system on channel connectivity. The formula is as follows:

$$R = \sum_{i=1}^{n} \frac{S_i}{S(n_i + 1)} \tag{3}$$

where R is the channel connectivity index, S is the total length of the channel(m), S_i is the length of the branch ditch i(m), and n_i is the number of check dams on the branch ditch i. The value range of R is 0 to 1, with a value closer to 1 indicating increased channel connectivity.

(2) Flow velocity (V). Velocity is an important hydraulic parameter in runoff erosion dynamics and sediment transport. Because of the uncertainty of the measured velocity, the discharge of the section is obtained by solving the Saint–Venant equation, and then the average velocity of the section is obtained by dividing the measured area of the section as follows:

$$V = Q/A \tag{4}$$

where V is the average velocity of the section (m s^{-1}), Q is the discharge of the section (m^3.s^{-1}), and A represents the measured sectional area (m^2).

(3) Runoff shear stress (τ). Runoff shear stress is a parameter reflecting the amount of soil erosion force exerted by runoff during flow. Foster et al. [42] proposed the formula of runoff shear stress as follows:

$$\tau = \gamma RJ \tag{5}$$

where τ is the runoff shear stress (N m^{-2}), γ is the bulk density of the runoff (N m^{-3}), R is hydraulic radius (m), and J is the hydraulic energy slope.

(4) Runoff erosion power (E). Runoff depth and flood peak flow are two important parameters reflecting the characteristics of storm flood process in the watershed. The product of runoff depth and flood peak flow indirectly reflects the spatial and temporal distribution characteristics of rainfall and the influence of the watershed underlying the surface on runoff confluence processes. The formula for calculating runoff erosion power is defined as [43]:

$$E = Q'_m H \tag{6}$$

where E is runoff erosion power (m^4 s^{-1} km^{-2}), H is the average runoff depth of the rainstorm(m), and Q'_m is the peak flow modulus (m^3 s^{-1} km^{-2}).

3. Results

3.1. Variation Characteristics of Rainstorm and Flood Process in Small Watershed under Different Working Conditions

The flood process of the small watershed changed under the eight working conditions of different dam combinations. Before the channel dam construction, the flood process of the small watershed rose and fell sharply, but this slowed down after dam construction. Comparing different working conditions of the flood process hydrographs of no dams (N), only key dams (K), only medium dams (M), and only small dams (S) revealed that all three kinds of dams reduced the peak discharge and flood volume, but different dam types had different effects on flood regulation (Figure 3). To quantitatively explain the influence of different dam type combinations on rainstorm flood processes in the small watershed, the flood characteristic parameters under different working conditions were analyzed. As shown in Table 3, construction of the dam system (KMS) will reduce the flood peak by 65.34% and the flood volume by 58.67%, resulting in the strongest flood control ability. When there are only key dams in the watershed, the flood peak and the flood volume will be reduced by 27.28% and 2.18%, resulting in a reduction in the flood peak that is far greater than that of the flood volume, indicating that the role of the key dam is mainly to regulate the flood process. While construction of only medium or small dams in the watershed will reduce the flood peak by 33.39% and 40.13% and the flood volume by 27.08% and 44.89%, respectively, resulting in a reduction in flood peak that is roughly the same as that of the flood volume. This indicates that medium and small dams not only regulate flood processes, but also reduce flood volume.

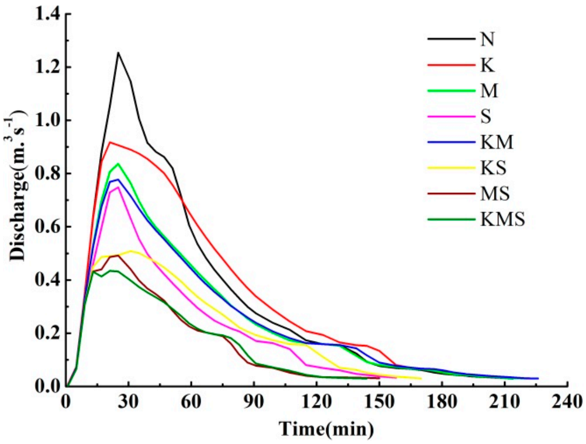

Figure 3. Simulation results under different working conditions.

Table 3. Flood characteristic parameters under different working conditions.

Working Conditions	Flood Peak Discharge (m^3 s^{-1})	Flood Peak Reduction (%)	Flood Volume (m^3)	Flood Volume Reduction (%)
N	1.26	-	4853.93	-
K	0.92	27.28	4828.87	2.18
M	0.84	33.39	3556.61	27.08
S	0.76	40.13	2541.04	44.89
KM	0.78	38.07	3532.24	27.37
KS	0.51	59.71	2518.06	45.15
MS	0.50	60.75	1802.36	58.42
KMS	0.44	65.34	1779.58	58.67

3.2. Variation of Dynamic Parameters of Channel Erosion under Different Working Conditions

In this study, two erosion dynamic parameters, velocity and runoff shear stress along the main channel section, were selected for analysis. There are four check dams in the main channel, Wangmaogou dam #2, Guandigou dam #1, Guandigou dam #2, and Guandigou dam #4, which have chainages of 2050, 1261, 733, and 529 m, respectively. Velocity is the most basic hydraulic parameter influencing runoff erosion and sediment transport. As shown in Figure 4a, the velocity of the cross section of the eight working conditions shows an increasing trend from upstream to the downstream portion of the main channel, although some sections tended to decrease. This is because the potential energy is gradually converted into kinetic energy during the downward movement of water along the channel, and the incoming water from the branch ditch continuously flows into the main channel so that the velocity is generally increasing. The reason for the sharp decrease between some sections is that the construction of check dams between these sections significantly reduced the velocity behind the dam. Comparison of the eight working conditions, the velocity along each section of the working condition N reaches the maximum, while the working condition KMS is the minimum, and that of the other working conditions were between these two conditions, indicating that the velocity along the main channel was reduced and the erosion of the channel by runoff was weakened after the dam system was completed. As shown in Figure 4b, the runoff shear stress of the eight working conditions first increased, then decreased, and the runoff shear stress of the section with the chainage of 1600–3800 m was greater than that of the section with the chainage of 0–1600 m. Comparison of the eight working conditions, the runoff shear stress of each section along working condition N was largest, while it was smallest along working condition KMS, and the other working conditions were between these two conditions. These findings indicate that completion of the dam system reduces the runoff shear stress along the channel. Overall, the erosion dynamic distribution of the main channel in the small watershed was changed to different extents by different dam type combinations, and the erosion dynamic parameters of the channel decreased most after the dam system was completed (KMS), when the maximum velocity and runoff shear stress of the outlet section were reduced by 10.69% and 31.08%, respectively (Table 4).

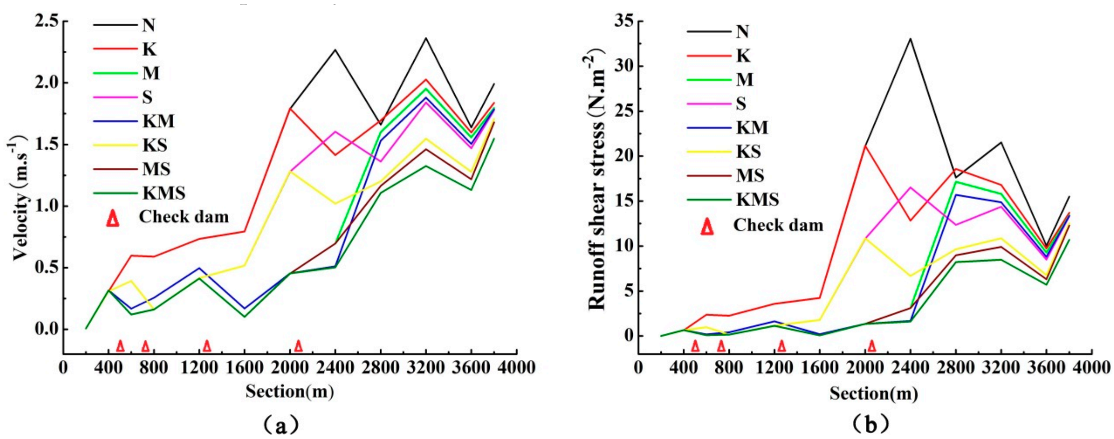

Figure 4. Distribution of erosion dynamic parameters along the channel under different working conditions.

Table 4. Erosion dynamic parameters of the exit section of the watershed under different working conditions.

Working Conditions	Velocity (m s^{-1})	Velocity Reduction (%)	Runoff Shear Stress (N S^{-2})	Runoff Shear Stress Reduction (%)
N	1.99	—	15.51	—
K	1.84	7.64	13.71	11.61
M	1.80	9.70	13.45	13.31
S	1.78	10.65	13.31	14.20
KM	1.79	10.30	13.36	13.89
KS	1.71	14.22	12.54	19.17
MS	1.68	15.58	12.27	20.86
KMS	1.55	22.26	10.69	31.08

3.3. Variation of Runoff Erosion Power along the Channel under Different Working Conditions

Runoff erosion power, as an important index of erosion and sediment yield of floods associated with a single storm, reflects the erosion dynamics in a watershed controlled by different sections. The runoff erosion power of different sections of the main channel of the basin was calculated using Formula (6). As shown in Figure 5, the runoff erosion power of each section along the working condition N was the largest, while that along the working condition KMS was smallest, and the other working conditions fell between these two conditions, indicating that the reduction extent of the runoff erosion power of the watershed was highest after the dam system was completed. Because the construction of check dams has no effect on the erosion dynamic process in slope, it mainly reduces the erosion power of the channel. Under eight working conditions, the runoff erosion power fluctuated greatly in the upper and middle reaches, while it remained basically the same in the lower reaches (less than 2800 m in mileage), and the erosion power of the lower reaches was less than that of the upper reaches, demonstrating that the upstream erosion is stronger and the downstream erosion is weaker, with a basically stable state. According to the Bagnold sediment transport rate, larger velocity and shear stress were associated with a greater sediment transporting capacity of a channel [44]. The velocity and runoff shear stress in the lower reaches of the Wangmaogou were higher than those in the upper reaches, which explains why the sediment transporting capacity of the downstream of the main channel is greater than that of the upstream. Overall, the characteristics of sediment yield and transport in the Wangmaogou watershed were as follows: The erosion of upstream branch ditches is intense, which focused on erosion and sediment yield, while the main channel erosion is weak, which was primarily a result of sediment transportation in gullies.

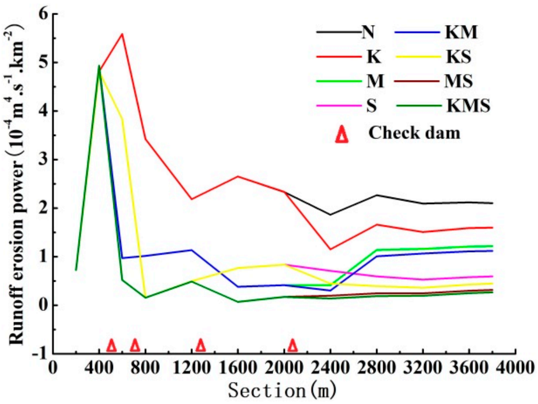

Figure 5. Distribution of runoff erosion power along the channel under different working conditions.

3.4. Impact of Different Dam Type Combinations on Sediment Discharge in Small Watershed

Runoff erosion power can better reflect erosion and sediment yield in watersheds. In the past, many scholars established regression equations between runoff erosion power and sediment transport moduli using a large amount of measured data that can be used to predict sediment yield in a watershed [45,46]. Based on the data describing the individual rainfall runoff and sediment measured from 1961 to 1964 at the watershed outlet hydrologic station in Wangaogou, the runoff depth, flood peak discharge modulus, and sediment transport modulus of individual floods in the basin during the period mentioned above were analyzed and counted, and the corresponding runoff erosion power was calculated. The runoff erosion power and sediment transport modulus of all floods in Wangaogou from 1961 to 1964 were plotted in a logarithmic coordinate system, and regression analysis was conducted (Figure 6), which resulted in establishment of a regression equation describing the runoff erosion power and sediment transport modulus of individual rainstorms and floods during the study period:

$$M_s = 701157P^{0.889}(R^2 = 0.89, n = 23) \tag{7}$$

where, M_s is the sediment transport modulus of an individual rainstorm, t km^{-2}; P is the runoff erosion power of an individual rainstorm, m^4 s^{-1} km^{-2}; and n *i*s the individual rainstorm flood time.

The sediment transport modulus of the watershed under eight working conditions was calculated according to Formula (7), and the results are shown in Table 5. The sediment transport modulus of the watershed reached 314.99 t.km^{-2} under working condition N and 50.66 t/km^2 under working condition KMS, while the values of other working conditions fell between these. When compared to no dam construction, the sediment transport modulus was reduced by 83.92% after the dam system was completed, indicating that the sediment transport modulus of the small watershed was reduced sharply because of completion of the dam system completion, and a large amount of sediment was intercepted in the system, which effectively reduces the sediment in the drainage ditch. Compared with working condition N, working condition K, M, and S reduced the sediment transport modulus in the watershed by 24.74%, 47.11%, and 64.11%, respectively, among which the sediment reduction benefit of small dams was the most obvious. When a number of small and medium dams were present, there was no water release structure, so that the incoming water and sand in the dam control area were completely blocked and stored.

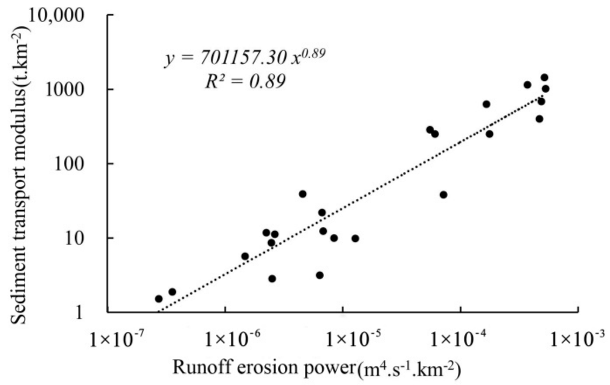

Figure 6. Relationship between runoff erosion power and sediment transport modulus of individual storms in the Wangmaogou watershed.

Table 5. Calculated sediment transport modulus for different dam type combinations.

Working Conditions	Flood Peak ($m^3\ s^{-1}$)	Flood Volume (m^3)	Runoff Erosion Power ($m^4\ s^{-1}\ km^{-2}$)	Sediment Transport Modulus ($t\ km^{-2}$)	Sediment Transport Modulus Reduction (%)
N	1.26	4853.93	1.72×10^{-4}	314.99	-
K	0.92	4828.87	1.25×10^{-4}	237.07	24.74
M	0.84	3556.61	8.38×10^{-5}	166.61	47.11
S	0.76	2541.04	5.42×10^{-5}	113.04	64.11
KM	0.78	3532.24	7.73×10^{-5}	155.03	50.78
KS	0.51	2518.06	3.60×10^{-5}	78.65	75.03
MS	0.50	1802.36	2.53×10^{-5}	57.41	81.78
KMS	0.44	1779.58	2.20×10^{-5}	50.66	83.92

4. Discussion

4.1. Impact of Check Dam System on Flood Processes in Small Watershed

The effects of individual rainstorm floods in the watershed were significantly changed by check dams through flood storage [13]. Construction of small dams had the greatest influence on flood processes, followed by medium and then key dams. This was primarily a result of the structural characteristics of these three types of dams [47]. There are no water release structures for small dams. Small check dams can completely block and store the interval and upstream inflow [48]. Therefore, as long as the dam does not break, the flood water will not pass, resulting in the greatest reduction in flood peak and flood volume. Medium dams are generally equipped with a horizontal tube or shaft and other drainage structures used for flood discharge. Key dams are not only equipped with water release structures, but also with spillways, which can discharge floodwater with time. As a result, key dams lead to a minimal reduction in flood peak and flood volume; however, they play important roles in protection of medium and small dams in a watershed dam system. To further analyze the action mechanism of the different dam type combinations on flood processes, the connectivity index (Table 6) of eight different dam combinations was calculated using Formula (3). The channel connectivity was reduced by 79.0% when the dam system was completed. Figure 7 shows the coefficient of determination for the relationship between the channel connectivity index and peak flow and total flood volume. As shown in the diagram, the difference between the channel connectivity index and the peak flow was as high as 0.97, and the correlation coefficient with the total flood volume was 0.89. There were close relationships between the channel connectivity index and peak flow and total flood volume, which indicate that the dam system layout adjusts the rainstorm flood process by changing the channel connectivity.

Table 6. Channel connectivity index under different working conditions.

\	Channel Connectivity Index	Flood Peak Discharge (m^3 s^{-1})	Flood Volume (m^3)
N	1	1.26	4853.93
K	0.70	0.92	4828.87
M	0.58	0.84	3556.61
S	0.39	0.76	2541.04
KM	0.52	0.78	3532.24
KS	0.28	0.51	2518.06
MS	0.26	0.50	1802.36
KMS	0.21	0.44	1779.58

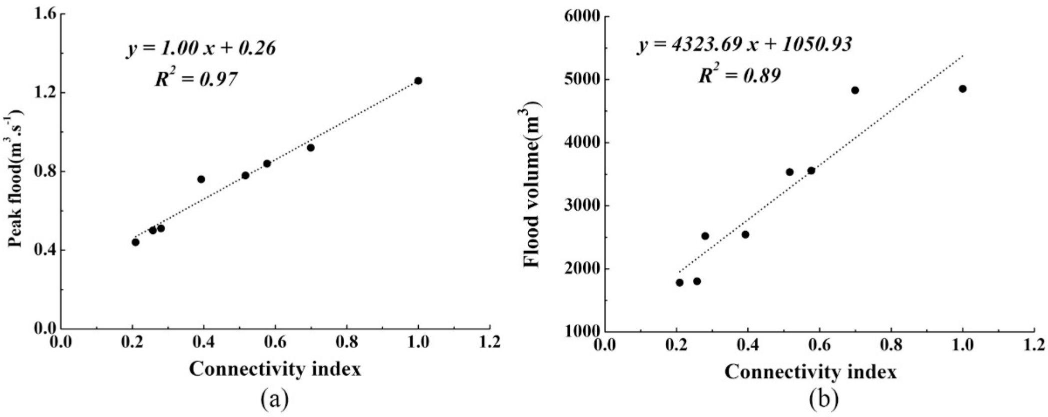

Figure 7. Relationships between channel connectivity index and peak flow (**a**); relationships between channel connectivity index and flood volume (**b**).

4.2. Impact of Check Dam System on Erosion Dynamics Process in Small Watershed

Runoff and sediment yield are extremely complex physical processes caused by the interaction between precipitation and the underlying surface of the basin [49]. Under the condition of individual rainstorms, the final result of their interaction is the flood characteristics of the watershed outlet, which can indirectly reflect the comprehensive influence of precipitation and underlying surface characteristics on the erosion and sediment yield of watershed. Runoff depth and peak discharge are two important parameters that reflect the characteristics of the individual rainstorm flood process in the basin. Runoff depth represents the total amount of flooding produced by an individual rainstorm, which reflects the precipitation amount and the redistribution impact of the different underlying surfaces on precipitation in the basin [50]. The peak discharge represents the flood intensity, which reflects the characteristics of temporal and spatial distribution of precipitation and the influence of the basin underlying surface on runoff confluence processes [51]. The runoff depth and peak discharge reflect some characteristics of the individual rainstorm flood, and cannot comprehensively reflect the effect on erosion and sediment yield. Therefore, the influence of different dam type combinations on erosion and sediment yield is analyzed by calculating the erosion power of individual rainstorm runoff, which shows that the runoff erosion power in the lower reaches of the basin is lower than that in the upper reaches. The results of some studies have shown that the runoff erosion power in the Yanhe Basin is large in upstream areas and small in downstream reaches [52], which is consistent with the results of the present study. The area of the Yanhe Basin is 7725 km^2, whereas that of Wangmaogou watershed is only 5.97 km^2. Even though the two basins have a huge difference in area, the runoff erosion power shows the same characteristics, indicating that the distribution of runoff erosion power depends not on the watershed area, but rather on the convergence process of rainfall runoff. The erosion characteristics of the Wangmaogou watershed were as follows: The erosion of upstream branch ditches is intense, resulting in erosion and sediment yield, while the main channel erosion is weak, mainly resulting in sediment transportation in gullies, which is consistent with the research results reported by Liao [53].

Figure 8 is the siltation modulus diagram of Wangmaogou watershed, from which it can be seen that the siltation modulus of the branch ditches in the upstream area is obviously larger than that of the main ditch in the downstream area, which also indirectly explains the conclusions above.

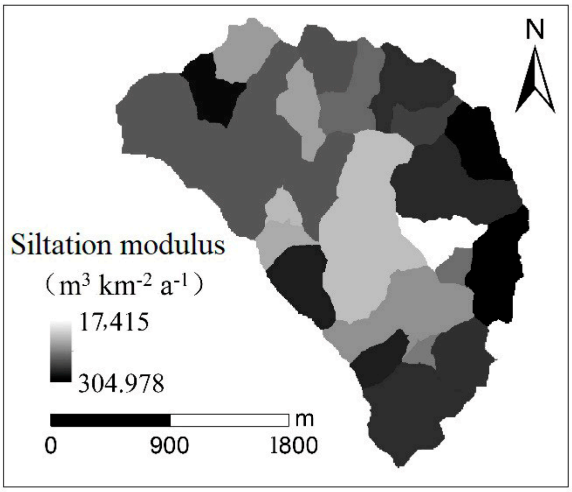

Figure 8. Siltation modulus diagram of the Wangmaogou watershed.

5. Conclusions

In this study, the hydrodynamic processes of the Wangmaogou watershed located in the Loess Plateau were simulated and the influence of check dam construction on the flood and erosion dynamic process in this small watershed was evaluated. The check dams reduced the flood peak and flood volume and mitigated the flood process, while different types of check dams played various roles in flood regulation. After the dam system was completed, the flood peak and flood volume were reduced by 65.34% and 58.67%, respectively. The erosion dynamic distribution of the main channel in the small watershed was changed, to different extents, by the different dam type combinations, and the erosion dynamic parameters of the channel decreased most after the dam system was completed, when the velocity and runoff shear stress of the outlet section were reduced by 10.69% and 31.08%, respectively. Under different dam type combinations, the runoff erosion power fluctuates greatly in the upper and middle reaches, while it remains basically the same in the lower reaches, and the erosion power of the downstream becomes lower than that of the upstream portion. Check dam construction can effectively reduce the sediment transport capacity in the watershed. When compared with the absence of dams in the basin, the sediment transport modulus of the key, medium, and small dams was reduced by 24.74%, 47.11%, and 64.11%, respectively, with the largest amplitude reduction being observed for small dams. The benefits of sediment reduction are most obvious after the check dam system is completed, with the sediment discharge in the basin being reduced by 83.92%.

Author Contributions: Conceptualization, S.Y. and Z.L.; methodology, P.L. and G.X.; formal analysis, H.G. and L.X.; software, F.W. and T.W.; S.Y. wrote the manuscript and all authors contributed to improving the paper.

Funding: This study was supported by the National Key Research and Development Program of China (2016YFC0402404), the National Natural Science Foundation of China (51779204, 41731289), the Consultation and Evaluation Project of the Chinese Academy of Sciences (2018-Z02-A-008), and the School Foundation of Xi'an University of Technology (310-252071711).

Acknowledgments: We thank the reviewers for their useful comments and suggestions.

Conflicts of Interest: The authors declare no conflicts of interest.

References

1. Pal, D.; Galelli, S.; Tang, H.; Ran, Q. Toward improved design of check dam systems: A case study in the Loess Plateau, China. *J. Hydrol.* **2018**, *559*, 762–773. [CrossRef]
2. Zhao, G.; Kondolf, G.M.; Mu, X.; Han, M.; He, Z.; Rubin, Z.; Wang, F.; Gao, P.; Sun, W. Sediment yield reduction associated with land use changes and check dams in a catchment of the Loess Plateau, China. *CATENA* **2017**, *148*, 126–137. [CrossRef]
3. Zhou, Z.; Li, J. The correlation analysis on the landscape pattern index and hydrological processes in the Yanhe watershed, China. *J. Hydrol.* **2015**, *524*, 417–426. [CrossRef]
4. Li, X.-G.; Wei, X. Soil erosion analysis of human influence on the controlled basin system of check dams in small watersheds of the Loess Plateau, China. *Expert Syst. Appl.* **2011**, *38*, 4228–4233. [CrossRef]
5. Shi, H.; Shao, M. Soil and water loss from the Loess Plateau in China. *J. Arid Environ.* **2000**, *45*, 9–20. [CrossRef]
6. Ran, D.-C.; Luo, Q.-H.; Zhou, Z.-H.; Wang, G.-Q.; Zhang, X.-H. Sediment retention by check dams in the Hekouzhen-Longmen Section of the Yellow River. *Int. J. Sediment Res.* **2008**, *23*, 159–166. [CrossRef]
7. Li, P.; Xu, G.; Lu, K.; Zhang, X.; Shi, P.; Bai, L.; Ren, Z.; Pang, G.; Xiao, L.; Gao, H.; et al. Runoff change and sediment source during rainstorms in an ecologically constructed watershed on the Loess Plateau, China. *Sci. Total Environ.* **2019**, *664*, 968–974. [CrossRef]
8. Vaezi, A.R.; Abbasi, M.; Keesstra, S.; Cerdà, A. Assessment of soil particle erodibility and sediment trapping using check dams in small semi-arid catchments. *CATENA* **2017**, *157*, 227–240. [CrossRef]
9. Shi, P.; Zhang, Y.; Ren, Z.; Yu, Y.; Li, P.; Gong, J. Land-use changes and check dams reducing runoff and sediment yield on the Loess Plateau of China. *Sci. Total Environ.* **2019**, *664*, 984–994. [CrossRef] [PubMed]
10. Jin, Z.; Cui, B.; Song, Y.; Shi, W.; Wang, K.; Wang, Y.; Liang, J. How Many Check Dams Do We Need To Build on the Loess Plateau? *Environ. Sci. Technol.* **2012**, *46*, 8527–8528. [CrossRef]
11. Guyassa, E.; Frankl, A.; Zenebe, A.; Poesen, J.; Nyssen, J. Effects of check dams on runoff characteristics along gully reaches, the case of Northern Ethiopia. *J. Hydrol.* **2017**, *545*, 299–309. [CrossRef]
12. Boix-Fayos, C.; Barberá, G.G.; López-Bermúdez, F.; Castillo, V. Effects of check dams, reforestation and land-use changes on river channel morphology: Case study of the Rogativa catchment (Murcia, Spain). *Geomorphology* **2007**, *91*, 103–123. [CrossRef]
13. Castillo, V.; Mosch, W.; García, C.C.; Barberá, G.G.; Cano, J.N.; López-Bermúdez, F.; Cano, J.A.N. Effectiveness and geomorphological impacts of check dams for soil erosion control in a semiarid Mediterranean catchment: El Cárcavo (Murcia, Spain). *CATENA* **2007**, *70*, 416–427. [CrossRef]
14. Hassanli, A.M.; Nameghi, A.E.; Beecham, S. Evaluation of the effect of porous check dam location on fine sediment retention (a case study). *Environ. Monit. Assess.* **2009**, *152*, 319–326. [CrossRef]
15. Bombino, G.; Gurnell, A.M.; Tamburino, V.; Zema, D.A.; Zimbone, S.M. Adjustments in channel form, sediment calibre and vegetation around check-dams in the headwater reaches of mountain torrents, Calabria, Italy. *Earth Surf. Process. Landf.* **2010**, *34*, 1011–1021. [CrossRef]
16. Leigh, D.S.; Kowalewski, S.A.; Holdridge, G. 3400 years of agricultural engineering in Mesoamerica: lama-bordos of the Mixteca Alta, Oaxaca, Mexico. *J. Archaeol. Sci.* **2013**, *40*, 4107–4111. [CrossRef]
17. Castillo, C.; Pérez, R.; Gomez, J.A.; Rodríguez, C.C. A conceptual model of check dam hydraulics for gully control: efficiency, optimal spacing and relation with step-pools. *Hydrol. Earth Syst. Sci.* **2014**, *18*, 1705–1721. [CrossRef]
18. Mekonnen, M.; Keesstra, S.D.; Stroosnijder, L.; Baartman, J.E.; Maroulis, J. Soil Conservation Through Sediment Trapping: A Review. *Land Degrad. Dev.* **2015**, *26*, 544–556. [CrossRef]
19. Xu, Y.D.; Fu, B.J.; He, C.S. Assessing the hydrological effect of the check dams in the Loess Plateau, China, by model simulations. *Hydrol. Earth Syst. Sci.* **2013**, *17*, 2185–2193. [CrossRef]
20. Boixfayos, C.; De Vente, J.; Martínez-Mena, M.; Barberá, G.G.; Castillo, V. The impact of land use change and check-dams on catchment sediment yield. *Hydrol. Process.* **2010**, *22*, 4922–4935. [CrossRef]
21. Kondolf, G.; Piégay, H.; Landon, N. Channel response to increased and decreased bedload supply from land use change: contrasts between two catchments. *Geomorphology* **2002**, *45*, 35–51. [CrossRef]
22. Mishra, A.; Froebrich, J.; Gassman, P.W. Evaluation of the SWAT Model for Assessing Sediment Control Structures in a Small Watershed in India. *Trans. ASABE* **2007**, *50*, 469–477. [CrossRef]

23. Xu, X.-Z.; Zhang, H.-W.; Zhang, O. Development of check-dam systems in gullies on the Loess Plateau, China. *Environ. Sci. Policy* **2004**, *7*, 79–86.
24. Lenzi, M.A.; Comiti, F. Local scouring and morphological adjustments in steep channels with check-dam sequences. *Geomorphology* **2003**, *55*, 97–109. [CrossRef]
25. Bracken, L.; Wainwright, J.; Parsons, A.J.; Poeppl, R.E.; Keesstra, S.D. Introduction to special issue on connectivity in water and sediment dynamics. *Earth Surf. Process. Landf.* **2015**, *40*, 1275–1277.
26. Romero-Díaz, A.; Marín-Sanleandro, P.; Ortiz-Silla, R. Loss of soil fertility estimated from sediment trapped in check dams. South-eastern Spain. *CATENA* **2012**, *99*, 42–53.
27. Quiñonero-Rubio, J.M.; Nadeu, E.; Boix-Fayos, C.; de Vente, J. Evaluation of the Effectiveness of Forest Restoration and Check-Dams to Reduce Catchment Sediment Yield. *Land Degrad. Dev.* **2016**, *27*, 1018–1031. [CrossRef]
28. Zema, D.A.; Bombino, G.; Denisi, P.; Lucas-Borja, M.E.; Zimbone, S.M. Evaluating the effects of check dams on channel geometry, bed sediment size and riparian vegetation in Mediterranean mountain torrents. *Sci. Total Environ.* **2018**, *642*, 327–340. [CrossRef] [PubMed]
29. Xu, G.; Cheng, S.; Li, P.; Li, Z.; Gao, H.; Yu, K.; Lu, K.; Shi, P.; Cheng, Y.; Zhao, B. Soil total nitrogen sources on dammed farmland under the condition of ecological construction in a small watershed on the Loess Plateau, China. *Ecol. Eng.* **2018**, *121*, 19–25. [CrossRef]
30. Zhao, B.; Li, Z.; Li, P.; Xu, G.; Gao, H.; Cheng, Y.; Chang, E.; Yuan, S.; Zhang, Y.; Feng, Z. Spatial distribution of soil organic carbon and its influencing factors under the condition of ecological construction in a hilly-gully watershed of the Loess Plateau, China. *Geoderma* **2017**, *296*, 10–17. [CrossRef]
31. Qin, C.-Z.; Ai, B.-B.; Zhu, A.-X.; Liu, J.-Z. An efficient method for applying a differential equation to deriving the spatial distribution of specific catchment area from gridded digital elevation models. *Comput. Geosci.* **2017**, *100*, 94–102. [CrossRef]
32. Guo, D.; Westra, S.; Maier, H.R. Impact of evapotranspiration process representation on runoff projections from conceptual rainfall-runoff models. *Water Resour. Res.* **2016**, *53*, 435–454. [CrossRef]
33. Van Cuyk, S.; Siegrist, R.L. Virus removal within a soil infiltration zone as affected by effluent composition, application rate, and soil type. *Water Res.* **2007**, *41*, 699–709. [CrossRef]
34. Madsen, H. Parameter estimation in distributed hydrological catchment modelling using automatic calibration with multiple objectives. *Adv. Water Resour.* **2003**, *26*, 205–216. [CrossRef]
35. McMichael, C.E.; Hope, A.S.; Loaiciga, H.A. Distributed hydrological modelling in California semi-arid shrublands: MIKE SHE model calibration and uncertainty estimation. *J. Hydrol.* **2006**, *317*, 307–324. [CrossRef]
36. Cibin, R.; Sudheer, K.P.; Chaubey, I. Sensitivity and identifiability of stream flow generation parameters of the SWAT model. *Hydrol. Process.* **2010**, *24*, 1133–1148. [CrossRef]
37. Wu, Q.; Liu, S.; Cai, Y.; Li, X.; Jiang, Y. Improvement of hydrological model calibration by selecting multiple parameter ranges. *Hydrol. Earth Syst. Sci. Discuss.* **2016**, *21*, 1–24. [CrossRef]
38. Henriksen, H.J.; Troldborg, L.; Nyegaard, P.; Sonnenborg, T.O.; Refsgaard, J.C.; Madsen, B. Methodology for construction, calibration and validation of a national hydrological model for Denmark. *J. Hydrol.* **2003**, *280*, 52–71. [CrossRef]
39. Mo, X.; Pappenberger, F.; Beven, K.; Liu, S.; De Roo, A.; Lin, Z. Parameter conditioning and prediction uncertainties of the LISFLOOD-WB distributed hydrological model. *Hydrol. Sci. J.* **2006**, *51*, 45–65. [CrossRef]
40. Butts, M.B.; Payne, J.T.; Kristensen, M.; Madsen, H. An evaluation of the impact of model structure on hydrological modelling uncertainty for streamflow simulation. *J. Hydrol.* **2004**, *298*, 242–266. [CrossRef]
41. Hooke, J. Coarse sediment connectivity in river channel systems: a conceptual framework and methodology. *Geomorphology* **2003**, *56*, 79–94. [CrossRef]
42. Foster, G.R.; Huggins, L.F.; Meyer, L.D. A Laboratory Study of Rill Hydraulics: I. Velocity Relationships. *Trans. ASAE* **1984**, *27*, 790–796. [CrossRef]
43. Kexin, L.; Zhanbin, L.; Hua, J. Application of Runoff Erosion Power in the Calculation of Soil Erosion and Sediment Yield on Hillslopes. *J. Water Resour. Water Eng.* **2009**, *20*, 70–73. (In Chinese)
44. Suyanto; Rintis, H.; Rian, M.S.P. The Analysis of Sediment Transport Using Yang Method, Engelund-Hansen Method, and Bagnold Method in Bah Bolon River, Simalungun Regency of North Sumatera. *Appl. Mech. Mater.* **2016**, *845*, 30–34. [CrossRef]

45. Sun, Q.; Li, Z.; Yu, K.; Lu, K.; Tang, S. Parameters of sediment transport model for individual rainstorm in the Loess Hilly and Gully Region under changing environment. *Sci. Soil Water Conserv.* **2016**, *14*, 1–9. (In Chinese)
46. Zhang, L.-T.; Li, Z.-B.; Wang, H.; Xiao, J.-B. Influence of intra-event-based flood regime on sediment flow behavior from a typical agro-catchment of the Chinese Loess Plateau. *J. Hydrol.* **2016**, *538*, 71–81. [CrossRef]
47. Wei, X.; Li, X.; Wei, N. Fractal features of soil particle size distribution in layered sediments behind two check dams: Implications for the Loess Plateau, China. *Geomorphology* **2016**, *266*, 133–145. [CrossRef]
48. Yazdi, J.; Moghaddam, M.S.; Saghafian, B. Optimal Design of Check Dams in Mountainous Watersheds for Flood Mitigation. *Water Resour. Manag.* **2018**, *32*, 4793–4811. [CrossRef]
49. Fang, N.; Shi, Z.; Chen, F.; Zhang, H.; Wang, Y. Discharge and suspended sediment patterns in a small mountainous watershed with widely distributed rock fragments. *J. Hydrol.* **2015**, *528*, 238–248. [CrossRef]
50. Modrick, T.M.; Georgakakos, K.P. The character and causes of flash flood occurrence changes in mountainous small basins of Southern California under projected climatic change. *J. Hydrol. Reg. Stud.* **2015**, *3*, 312–336. [CrossRef]
51. Parsons, A.; Stone, P.; Parsons, A. Effects of intra-storm variations in rainfall intensity on interrill runoff and erosion. *CATENA* **2006**, *67*, 68–78. [CrossRef]
52. Gong, J.; Li, Z.; Li, P.; Ren, Z.; Yang, Y.; Han, L.; Tang, S.; Sun, Q. Spatial distribution of runoff erosion power based on SWAT Model in Yanhe River Basin. *Trans. Chin. Soc. Agric. Eng.* **2017**, *33*, 120–126. (In Chinese)
53. Liao, Y.S.; Cai, Q.G.; Zhuo, M.N.; Zheng, M.G.; Luo, X. Influence of Channel Networks on the Sediment Yield Under Variant Temporal and Spatial Scales:A Case Study of Chabagou Watershed. *Prog. Geogr.* **2009**, *28*, 47–54. (In Chinese)